480994

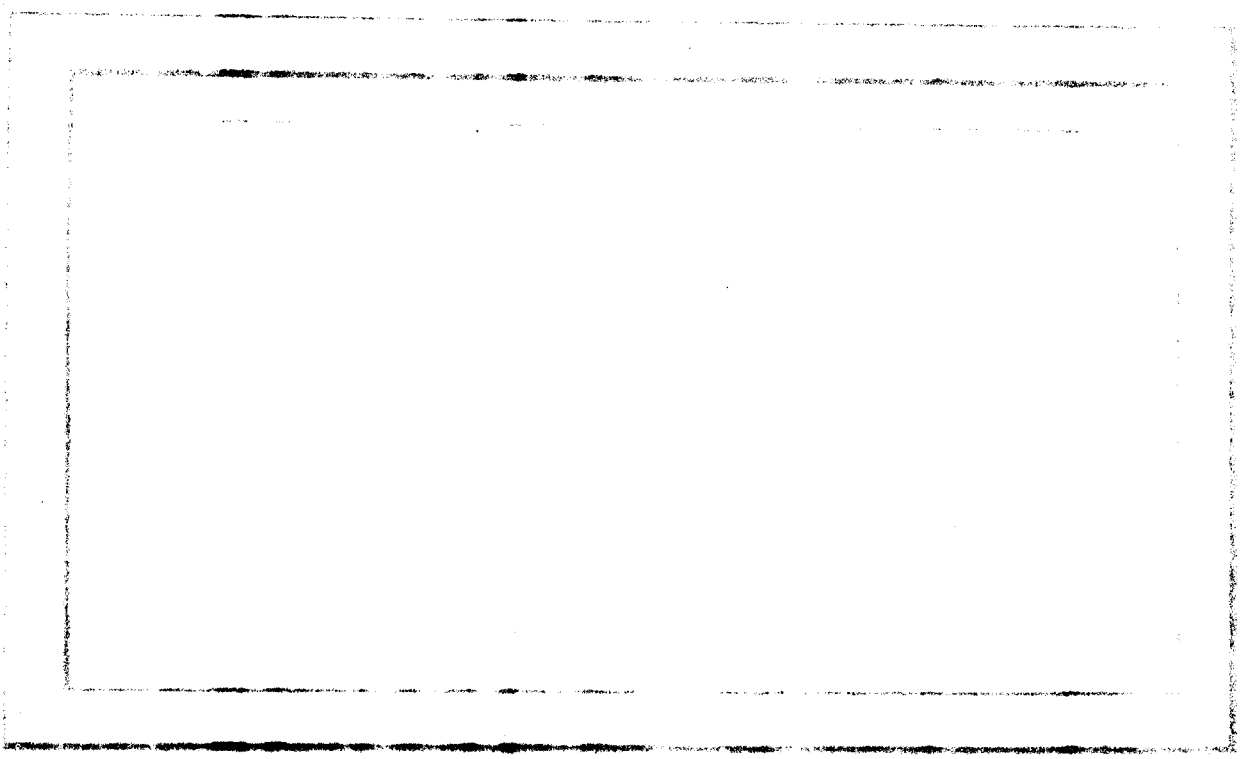

Therm
Advanced
Research, Inc.

[illegible] HUDSON CIRCLE • ITHACA, NEW YORK

A THREE-DIMENSIONAL THEORY FOR THE DUCTED PROPELLER AT ANGLE OF ATTACK

by

M. D. Greenberg, D. E. Ordway & C. F. Lo

TAR-TR 6509 December 1965

Submitted to

Air Programs, Office of Naval Research
Washington, D. C.

In partial fulfillment of Contract Nonr-4357(00)

Approved:

Alfred Ritter

Alfred Ritter,
President

ACKNOWLEDGMENT

The authors wish to acknowledge the extensive contribution to the analysis made by K. P. Kerney, during his Summer employment at TAR, Inc. The authors also wish to acknowledge the thorough review, checking and comments by J. C. Erickson, Jr., the helpful discussions and suggestions by A. Ritter and G. R. Hough, and the programming and calculations by A. L. Kaskel.

ABSTRACT

An inviscid theory is developed for the steady aerodynamic loading on a ducted propeller in forward flight at angle of attack. As a first approximation, the problem is regarded as the superposition of the given ducted propeller at zero incidence and a cylindrical duct of the same aspect ratio but of zero thickness and camber at the given incidence. This approximation is then improved to include the cyclic variation of the blade loading. Not only are the normal force and pitching moment changed but also a finite side force and yawing moment, unknown heretofore, are found. Explicit formulas are given to carry out numerical calculations and a limited comparison with experimental results show good agreement.

TABLE OF CONTENTS

PRINCIPAL NOMENCLATURE

a,b	unsteady airfoil coefficients; see Eqs. (45) and (58) and Table II
a_ν, b_ν	Glauert coefficients for $\sin\theta$ and $\cos\theta$ portions, respectively, of steady shroud vortex loading; see Eqs. (4), (49) and (50)
A,B	$\sin\theta$ and $\cos\theta$ portions of steady shroud vortex loading respectively; see Eq. (4)
c	shroud chord
c_p	shroud surface pressure coefficient; see Eq. (24)
c_{p_0}	axisymmetric portion of c_p, identical to c_p for zero incidence
c_ν	Glauert coefficients for axisymmetric portion of steady shroud vortex loading γ_0/U
$C_{(\ )}$	shroud and propeller force and moment coefficients; see Eqs. (31) and (32), for example
d	blade chord
f	shroud source strength per unit axial length
$\mathcal{f}_\nu, \mathcal{g}_\nu$	Fourier-type coefficients of $\mathcal{F}/\alpha$ and $\mathcal{G}/\alpha$ respectively; see Eqs. (51) and (52)
$\mathcal{F}, \mathcal{G}$	$\sin\theta$ and $\cos\theta$ portions, respectively, of steady radial velocity induced on shroud reference cylinder due to cyclic loading on propeller; see Eqs. (46) and (48)
J	propeller advance ratio, $U/\Omega R_p$
k	reduced frequency of sinusoidal inflow to propeller blade sections; see Eq. (44)
$\mathcal{K}$	kernel of integral equations for inclined duct problem; see Eqs. (6) and (19)
ℓ	blade index; $\ell = 0, 1, \ldots, (N-1)$
$\mathcal{l}$	shroud lift
L	propeller lift

$\mathcal{M}$	shroud pitching moment, positive nose-up
M	propeller pitching moment, positive nose-up
$\mathcal{N}$	shroud yawing moment, positive nose-right
N	number of propeller blades
N	propeller yawing moment, positive nose-right
$[\mathcal{O}]$	inversion matrix; see Eqs. (23), (53) and (54), and Tables 2 - 5
p	static pressure on shroud
p_∞	static pressure at infinity
$Q_{n+\frac{1}{2}}$	Legendre function of second kind and half order $(n+\frac{1}{2})$ with argument ω
R	reference radius, taken as mean shroud radius at propeller plane
R_p	propeller radius
$\mathcal{S}$	shroud side force, positive in positive y-direction
S	propeller side force, positive in positive y-direction
$[\mathcal{S}]$	extended Hough matrix; see Eq. (27) and Tables 6 - 9
t	time
t	shroud thickness distribution
u,v,w	steady x,r,θ-components of disturbance flow respectively
$\hat{u},\hat{v},\hat{w}$	unsteady x,r,θ-components of disturbance flow respectively
U	flight speed
$v_{f,\gamma,\ \ldots}$	steady portions of radial velocity induced by f,γ, ... respectively
v_{f_0,γ_0}	axisymmetric portions of $v_{f,\gamma}$ respectively
$\mathcal{W}$	resultant velocity $(U^2+\Omega^2r^2)^{\frac{1}{2}}$ relative to blade element

x, r, θ	shroud-fixed cylindrical coordinates; see Fig. 1
x, y, z	shroud-fixed Cartesian coordinates; see Fig. 1
x_p	axial propeller position, positive downstream of shroud midchord; see Fig. 1
$\bar{x}, \bar{r}$	x/R and r/R respectively
α	angle of attack to free stream, in radians
γ	total steady bound shroud vortex strength per unit axial length
γ_0, γ_1	axisymmetric and θ-dependent portions of γ respectively; see Eq. (4)
$\Gamma, \hat{\Gamma}_\ell$	steady and unsteady portions, respectively, of bound circulation distribution on ℓth blade
ϵ	local inclination angle of shroud camber line relative to x-axis; see Fig. 1
θ_ℓ	angular position of ℓth blade, $(-\Omega t + 2\pi\ell/N)$
ϑ, ϑ_b	phase angles for unsteady blade circulation and lift per unit length respectively; see Eqs. (41) and (43) and p. 27
λ	shroud chord-to-diameter ratio, c/2R
μ	R_p/R
Π_u, Π_w	inflow velocity factors; see Eqs. (36) - (38) and Table 10
σ, σ_b	amplitude factors for unsteady blade circulation and lift per unit length respectively; see Eqs. (41) and (42) and p. 27
ϕ	chordwise Glauert variable; $\bar{x} = -\lambda \cos \phi$
$\{\varphi\}, \{\phi\}$	column vectors associated with three-dimensional contribution to c_p ; see Eqs. (27) - (29) and (55)
Ω	angular rotational speed of propeller, radians per unit time

INTRODUCTION

In previous studies we have treated the ducted propeller extensively for the case of forward flight at zero incidence[1-4], as well as static and low-speed flight[5]. Here our attention is turned to the case of forward flight at angle of attack. We take the design propeller loading and the shroud geometry as known and seek to determine the steady part of the shroud loading.

Consider first the related problem of the isolated duct at angle of attack, which has been studied in detail by H. Ribner[6], J. Weissinger[7,8] and many others. From Weissinger's theory, the duct at incidence may be regarded as the superposition of the given duct at zero incidence, plus a cylinder of the same aspect ratio but of zero thickness and camber, at the given incidence. The results have been found to be in excellent agreement with experiment[9,10].

The ducted propeller at angle of attack, however, is considerably more difficult. This is clear at the outset on the basis of the difficulty encountered in dealing with the bare propeller at incidence[11,12]. A. R. Kriebel[13] has treated the problem by an a priori extension of the above superposition principle. That is, he regards the ducted propeller at incidence as the superposition of the given ducted propeller at zero incidence, plus a cylinder of the same aspect ratio but of zero thickness and camber at the given incidence. His approach does not seem too unreasonable and reduces the problem to the sum of two problems for which the solutions are available[4,8]. Unfortunately, though, it completely ignores the incidence of the flow to the propeller plane and hence the cyclic fluctuation of the circulation on the propeller. For a bare propeller this cyclic fluctuation causes additional steady loads. As a result, we expect similar loads for the ducted propeller, not only on the propeller itself but also on the duct due to its interaction with the propeller.

We start with a general formulation of the problem and then examine the superposition model as a first approximation. The cyclic fluctuation of the loading on the propeller and the associated interaction with the shroud follow and an improved solution together with illustrative results are found. In conclusion, comparison with some DTMB experiments are made.

CHAPTER ONE

GENERAL FORMULATION

1.1 Physical Model and Problem Statement

We consider a ducted propeller in steady forward flight U with a constant rotational propeller speed Ω and angle of attack α in an unbounded, inviscid, incompressible fluid otherwise at rest, see Fig. 1 . The coordinate system (x,r,θ) shown is fixed to the shroud. In our previous work[1,2] for the case of zero incidence, propeller-fixed coordinates were used since the flow was steady with respect to such a frame. In the present case, however, the flow is unsteady with respect to any reference frame and shroud-fixed coordinates are found to be more convenient.

We assume that both the angle of attack and the shroud camber are small. We also assume that the shroud thickness is small compared to the shroud chord c . The N propeller blades are taken to be slender and lightly loaded, and the hub is neglected. As a reference radius, we choose the radius R of the camber line at the propeller plane.

With these assumptions, we may represent the propeller by the classical lifting-line model wherein each blade is replaced with a single bound radial vortex and an accompanying helical sheet of trailing vortices. The situation is complicated, though, by the fact that the blade circulation must experience a cyclic fluctuation about its design, or mean, value due to the incidence of the ducted propeller to the free stream. Consequently, additional shed vortices enter the stream at, and parallel to, the lifting lines and convect downstream.

As in thin annular airfoil theory, a superposition of ring sources and bound ring vortices, together with an appropriate system of trailing vortices, is used for the shroud. Again, the situation is complicated by the addition of shed vortices since the bound vortex strength varies with time. This arises partly from the cyclic fluctuation in the propeller loading and partly from the change in the radial wash induced by the mean loading itself as the blades rotate.

With the above model in mind, the problem may be stated mathematically as follows: Given the geometry of the configuration and the mean propeller blade circulation, determine the shroud source distribution and the steady part of the bound shroud vortex distribution such that the tangent-flow condition is satisfied at the reference cylinder and the Kutta condition, at the trailing edge.

1.2 Tangent-Flow Condition

The linearized tangent-flow condition is well known and has the form given

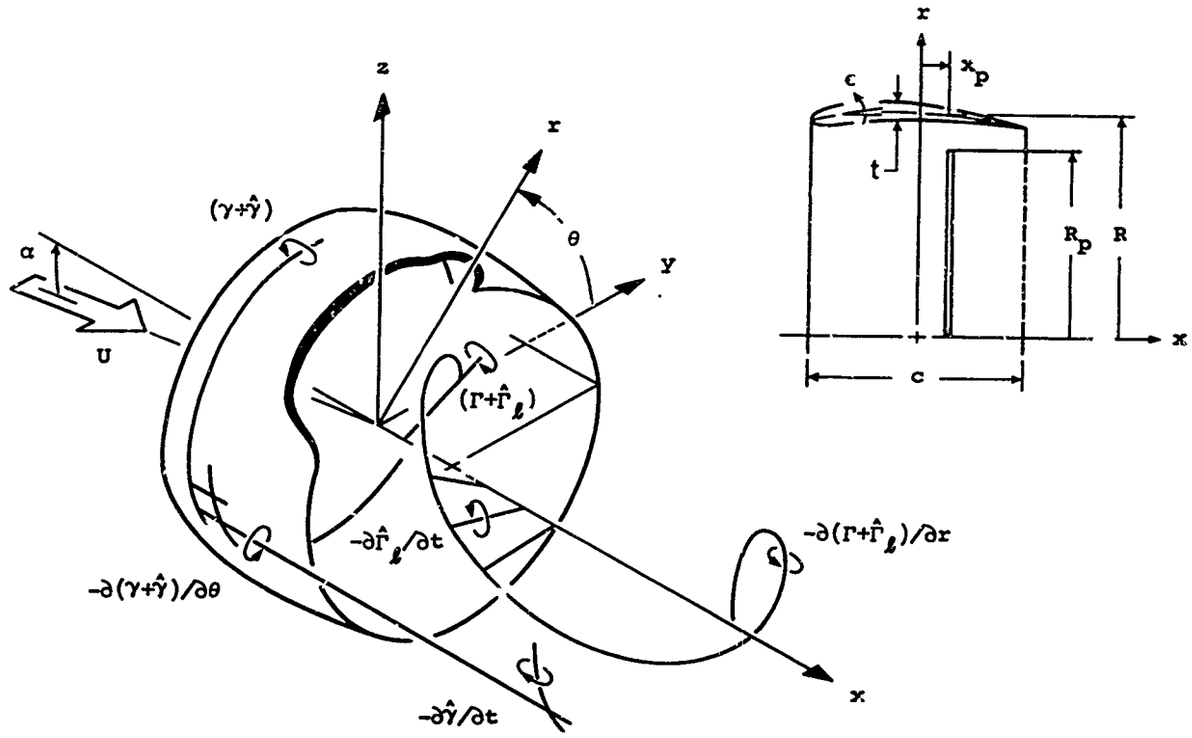

ω

FIGURE 1

GEOMETRY OF DUCTED PROPELLER CONFIGURATION

by

$$\epsilon \pm \frac{t'}{2} - \alpha \sin\theta = \frac{v}{U} \qquad -c/2 < x \leq c/2 \ , \ r = R\pm \tag{1}$$

where ϵ denotes the local inclination of the camber line to the x-axis, and t denotes the local shroud thickness, the prime indicating differentiation with respect to its argument x. In addition, we take u,v,w and $\hat{u},\hat{v},\hat{w}$ to be the steady and unsteady axial, radial and circumferential portions of the disturbance flow respectively. Eq. (1) is, in fact, only the steady part of the tangent-flow condition. The unsteady part is simply $0 = \hat{v}$ on the mean duct surface. Similarly, the steady and unsteady portions of the flow must satisfy the Kutta condition separately, since the total flow must satisfy the Kutta condition. In seeking the steady shroud loading we shall be concerned only with Eq. (1) together with its associated steady Kutta condition.

1.3 Evaluation of the Steady Radial Wash

The distribution of the shroud source and vortex strengths per unit length are taken to be f and $(\gamma + \hat{\gamma})$ respectively, and the bound circulation distribution over the ℓth blade is defined as $(\Gamma + \hat{\Gamma}_\ell)$. Of these, only Γ is specified a priori.

The trailing vortices from the shroud $-\partial(\gamma + \hat{\gamma})/\partial\theta$ are assumed to convect downstream with the speed U. Each bound ring vortex therefore contributes a semi-infinite cylinder of straight trailing vortices. The corresponding shed vortices $-\partial\hat{\gamma}/\partial t$ constitute a similar cylinder but composed of ring vortices.

The trailing vortices from the propeller $-\partial(\Gamma + \hat{\Gamma}_\ell)/\partial r$ are also assumed to convect downstream with the speed U and so form regular helices with advance ratio $U/\Omega r$. The shed vortices $-\partial\hat{\Gamma}_\ell/\partial t$ emitted from each blade fall on these helices and, as above, are perpendicular locally to the trailing vortices.

The steady radial wash v may be expressed accordingly as the superposition of the individual contributions, or

$$v = v_f + v_\gamma + v_{\hat{\gamma}} + v_{\gamma'} + v_{\hat{\gamma}'} + v_{\dot{\hat{\gamma}}} + v_\Gamma + v_{\hat{\Gamma}} + v_{\Gamma'} + v_{\hat{\Gamma}'} + v_{\dot{\hat{\Gamma}}} . \tag{2}$$

where the prime refers to the trailing vortices and the dot to the shed vortices; v_f is the steady radial wash induced by the source distribution, and so forth.

Now consider each contribution in turn. We know v_f is independent of θ and hence denote this fact by setting

$$v_f = v_{f_0} \tag{3}$$

This quantity is calculated explicitly in Ref. 3 , but for our purposes the above will suffice.

To evaluate the shroud vortex contributions, we take the steady part γ in the form,

$$\gamma \equiv \gamma_0 + \gamma_1$$

$$= UC + UA \sin\theta + UB \cos\theta \qquad (4)$$

with C , A and B as functions of x . The first two terms on the right hand side are required on the basis of the results for ring wings at incidence. The necessity of the additional cosine term will become apparant when we discuss the propeller term $v_{\hat{\gamma}}$. From the Biot-Savart law it can then be shown, cf. Ref. 1 , that $(v_\gamma + v_{\gamma'})$ is composed of an axisymmetric contribution from γ_0 , plus $\sin\theta$ and $\cos\theta$ contributions from γ_1 and $-\partial\gamma_1/\partial\theta$, or

$$v_\gamma + v_{\gamma'} = v_{\gamma_0}(\bar{x}) + U \sin\theta \int_{-\lambda}^{\lambda} \mathcal{K} A(\bar{x}_v)\, d\bar{x}_v + U \cos\theta \int_{-\lambda}^{\lambda} \mathcal{K} B(\bar{x}_v)\, d\bar{x}_v \qquad (5)$$

where $\bar{x} \equiv x/R$, $\Delta\bar{x}_v \equiv \bar{x} - \bar{x}_v$, $\lambda \equiv c/2R$ and

$$\mathcal{K} \equiv 1/4 + \Delta\bar{x}_v \left[-Q'_{\frac{1}{2}} - Q'_{-\frac{1}{2}} + Q_{\frac{1}{2}} + Q_{-\frac{1}{2}} \right] / 4\pi \qquad (6)$$

The Q's are Legendre functions of the second kind and order $3/2$, $-1/2$, $1/2$, $-1/2$ respectively, the primes denoting differentiation with respect to their argument,

$$\omega = 1 + (\Delta\bar{x}_v)^2/2 \qquad (7)$$

The Q' terms in $\mathcal{K}$ can be traced to the bound vortices of γ_1 and the other three terms to the corresponding trailing vortices of $-\partial\gamma_1/\partial\theta$.

Turning to the remaining shroud contributions to v due to the unsteady part $\hat{\gamma}$, we have

$$v_{\hat{\gamma}} = 0 \qquad (8)$$

$$v_{\hat{\gamma}'} = 0 \qquad (9)$$

$$v_{\hat{\gamma}_0} = 0 \qquad (10)$$

This follows immediately from a generalization of Eq. (5) for the expected form of $\hat{\gamma}$.

Finally, we take up the various propeller contributions. It is not difficult to prove that the bound contributions vanish, regardless of the form of Γ and $\hat{\Gamma}_\ell$,

$$v_\Gamma = 0 \tag{11}$$

$$v_{\hat{\Gamma}} = 0 \tag{12}$$

and that the trailing contribution $v_{\Gamma'}$ is independent of θ , so

$$v_{\Gamma'} = v_{\Gamma_0'}(\bar{x}) \tag{13}$$

This effective propeller induced camber is the same as for the case of zero incidence.

For the last two contributions, we assume $\hat{\Gamma}_\ell$ varies sinusoidally as Ωt since only the first "harmonic" is present in either the case of the duct at incidence or of the propeller at incidence. The amplitude and the phase angle are not known a priori, but must be determined by solving the unsteady propeller problem explicitly. However, they will be regarded as known quantities for the moment. From Biot-Savart integration then we find,

$$v_{\hat{\Gamma}'} = U \mathcal{F} \sin\theta + U \mathcal{G} \cos\theta \tag{14}$$

where $\mathcal{F}$ and $\mathcal{G}$ are functions of $\bar{x}$ involving complicated double integrals over the amplitude and phase angle of $\hat{\Gamma}_\ell$. Both $\mathcal{F}$ and $\mathcal{G}$ owe their presence to the helical nature of the propeller vortex system, cf. Ref. 2 , and tend to zero in the limit as the advance ratio of the propeller becomes infinite. They will be dealt with later.

This leaves only the shed term $v_{\hat{\Gamma}'}$ from the propeller. By means of the result for $v_{\hat{\Gamma}}$

$$v_{\hat{\Gamma}'} = 0 \tag{15}$$

That is, the shed vortex system may be interpreted as a sequence of propellers of incremental loading, displaced both axially and circumferentially downstream of the propeller plane, each one of which is governed by Eq. (12) .

1.4 θ-Decomposition of Tangent-Flow Condition

With v given by Eqs. (2), (3), (5) and (8) - (15) , the tangent-flow condition of Eq. (1) must be valid for like terms in θ . For the zeroth terms, we have

$$\epsilon \pm \frac{t'}{2} = (v_{f_0} + v_{\gamma_0} + v_{\Gamma_0'})/U \tag{16}$$

and for the $\sin\theta$ and $\cos\theta$ terms respectively,

$$-\alpha - \mathscr{F} = \int_{-\lambda}^{\lambda} \mathscr{K}(\Delta\bar{x}_v)\, A(\bar{x}_v)\, d\bar{x}_v \tag{17}$$

$$-\mathscr{G} = \int_{-\lambda}^{\lambda} \mathscr{K}(\Delta\bar{x}_v)\, B(\bar{x}_v)\, d\bar{x}_v \tag{18}$$

where $\mathscr{K}$ is the kernel. It is identical to our $-K_m'$ of Refs. 1 and 2 with $mN = 1$ and $U/\Omega R_p \to \infty$, which has been related to Weissinger's ring-wing kernel[7].

We see now that Eq. (16) represents the same ducted propeller configuration in forward flight at <u>zero</u> incidence. This equation has already been solved for the corresponding shroud vortex and source distributions in Refs. 3 and 4 . We therefore turn our attention to the "incidence" equations or Eqs. (17) and (18) . As we have said, both $\mathscr{F}$ and $\mathscr{G}$ depend on the amplitude factor and phase angle of the unsteady part of the propeller circulation. Since they are found to depend in turn on the unknowns A and B , these equations are coupled through $\mathscr{F}$ and $\mathscr{G}$.

CHAPTER TWO

SUPERPOSITION PRINCIPLE AS A FIRST APPROXIMATION

2.1 The Superposition Principle

It appears physically reasonable that as a first approximation A and B can be evaluated by using a simple superposition of the given ducted propeller at zero incidence plus a cylindrical duct at incidence α, see Fig. 2. In terms of our incidence equations, this is equivalent to neglecting both $\mathscr{F}$ and $\mathscr{G}$ entirely. Thus A is governed by the "inclined-duct equation",

$$-\alpha = \int_{-\lambda}^{\lambda} \mathscr{K}(\Delta\bar{x}_\nu)\, A(\bar{x}_\nu)\, d\bar{x}_\nu \tag{19}$$

and B is identically zero.

Although other results are available, we will outline a solution to Eq. (19), based upon our Legendre function formulation, which is more convenient for computation and for subsequent inclusion of the propeller interaction terms $\mathscr{F}$ and $\mathscr{G}$.

2.2 Solution for the Inclined Duct

We introduce the Glauert angular variable ϕ, $0 \leq \phi \leq \pi$, according to the relations,

$$\bar{x} \equiv -\lambda \cos\phi \quad , \quad \bar{x}_\nu \equiv -\lambda \cos\phi_\nu \tag{20}$$

and seek a Glauert series solution of the form

$$A = \alpha \left[a_0 \cot\frac{\phi}{2} + \sum_{\nu=1}^{\infty} a_\nu \sin\nu\phi \right] \tag{21}$$

which satisfies the Kutta condition at the trailing edge and has the proper square-root singularity at the leading edge.

As in the case of the ducted propeller at zero incidence, the kernel behaves as $1/2\pi\Delta\bar{x}_\nu$ as $\Delta\bar{x}_\nu \to 0$, or

$$\mathscr{K} \equiv 1/2\pi\Delta\bar{x}_\nu + \mathscr{R} \tag{22}$$

The regular part $\mathscr{R}$ is equal to $1/4$ plus an antisymmetric function of $\Delta\bar{x}_\nu$

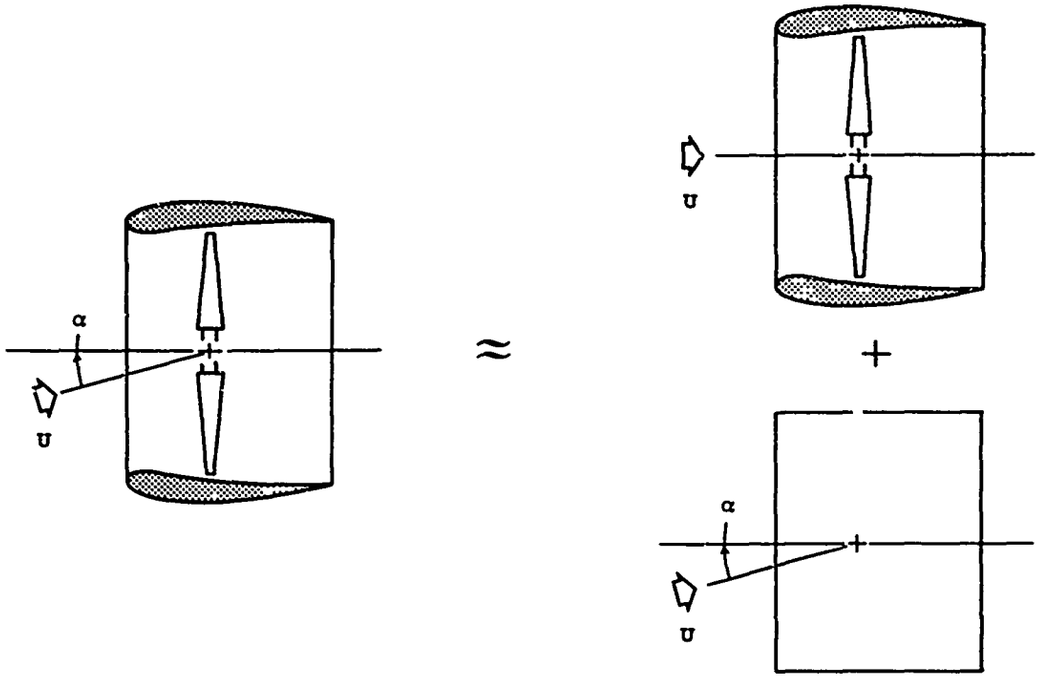

FIGURE 2

SUPERPOSITION PRINCIPLE FOR DUCTED PROPELLER AT ANGLE OF ATTACK

which approaches $1/4$ as $\Delta\bar{x}_\nu \to \infty$, see Fig. 3, and may be expanded in a double Fourier cosine series in ϕ, ϕ_ν. We have computed the first eight Fourier coefficients in each series numerically, for $\lambda = 0.25, 0.5, 0.75, 1.0$,

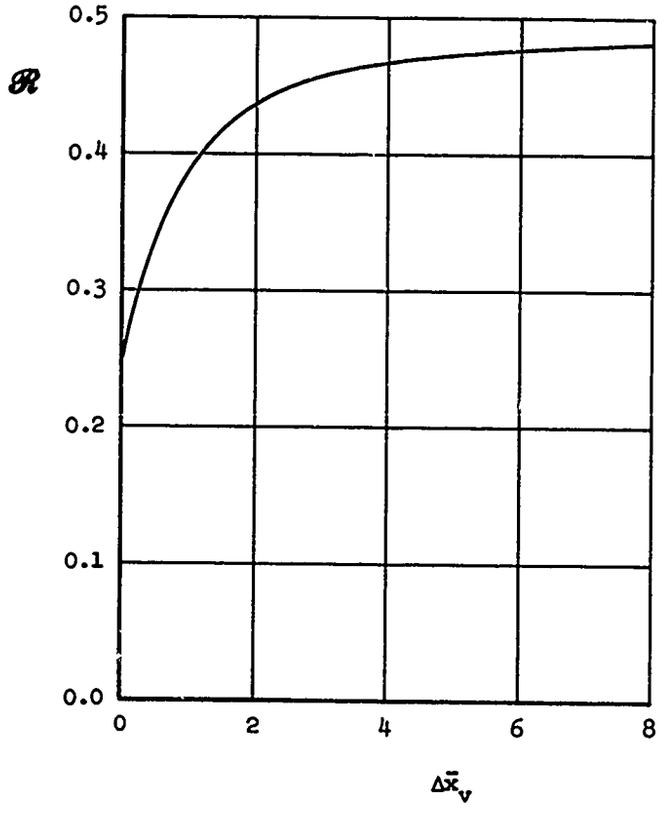

FIGURE 3

REGULAR PART OF THE KERNEL

to an accuracy of ± 1 in the fifth significant figure. These coefficients are related simply to Weissinger's $b_{\nu\mu}^{(1)}$ coefficients and agree well with the corresponding values that have been calculated by him* and the Bureau Technique Zborowski.

With $\mathscr{R}$ thus expressed, Eqs. (19) - (22) produce an infinite set of algebraic equations in the unknown Glauert coefficients. This set may be inverted

* The authors gratefully acknowledge numerical checks provided through private communication.

in the matrix form

$$\{a\} = -[\mathcal{O}]\ \{\,1\,,\,0\,,\,0\,,\,\ldots\,\}^{T} \tag{23}$$

where $\{a\}$ is a column vector with elements a_0, a_1, ..., and the inversion matrix $[\mathcal{O}]$ is an infinite square matrix with elements which depend on λ. Retaining only a_0 through a_6, we have inverted the truncated system numerically for $\lambda = 0.25, 0.5, 0.75, 1.0$ and have tabulated the resulting $\{a\}$ vectors in Table 1. The inversion matrix $[\mathcal{O}]$ is also given, in Tables 2-5, since it will be needed later in the analysis. For i or $j \geq 7$, the elements $\mathcal{O}_{i,j}$ may be approximated by their asymptotic values, $\mathcal{O}_{i,i} \sim 2.0$ and $\mathcal{O}_{i,j} \sim 0.0$ for $i \neq j$.

2.3 Shroud Surface Pressures

The steady shroud surface pressure coefficient is defined in the conventional form,

$$c_p \equiv \frac{p - p_\infty}{\frac{1}{2}\rho U^2} \tag{24}$$

where p is the steady static pressure on the shroud, p_∞ the static pressure at infinity, and ρ the fluid mass density. It follows from the linearized Bernoulli equation that

$$c_p = -2u/U \tag{25}$$

Within the superposition approximation, this may be rewritten as the sum of the pressure on the given ducted propeller at zero incidence, plus the pressure on the inclined duct, that is,

$$c_p = c_{p_0} - 2u_{\gamma_1}(\bar{x}, 1^{\pm}, \theta)/U \tag{26}$$

with $\gamma_1 = UA \sin\theta$. Only the bound vortices on the duct contribute to the inclined duct pressure since the trailing vortices are parallel to the x-axis and do not induce any axial component of velocity.

To calculate the axial velocity induced on the inclined duct, we first consider an arbitrary field point $(\bar{x}, \bar{r}, \theta)$ off the shroud and then let $\bar{r} \to 1^{\pm}$. In the limit, this reduces to the local "two-dimensional" value $\mp\frac{1}{2}$ UA sin θ plus a "three-dimensional" term. The three-dimensional term is equal to $U \sin\theta$ times the chordwise integral of $A(\bar{x}_v)$ weighted by $(Q'_{\frac{1}{2}} + Q'_{-\frac{1}{2}} - 2Q'_{\frac{1}{2}})/4\pi$, Eq. (7) giving the argument of the Q's.

It is convenient to express this result in matrix form for use in conjunction with $\{a\}$ from Eq. (23) . The matrix form of the two-dimensional part can be written down immediately. For the matrix form of the three-dimensional part, we follow Hough[3]. Thus Eq. (26) becomes

$$c_p = c_{p_0} + \alpha(\pm\{\varphi\}^T - \{\phi\}^T[\mathscr{S}]^T)\{a\}\sin\theta \tag{27}$$

where we have introduced the vectors,

$$\{\varphi\}^T \equiv \{\cot\tfrac{\phi}{2}\ ,\ \sin\phi\ ,\ \sin 2\phi\ ,\ \ldots\} \tag{28}$$

$$\{\phi\}^T \equiv \{1\ ,\ -\cos\phi\ ,\ -\cos 2\phi\ ,\ \ldots\} \tag{29}$$

Values of the vectors $\{\varphi\}$ for $x/c = -0.5, -0.4, \ldots 0.5$ respectively are given by the rows of the matrix composed of COLUMNS 118, 120, ... 130 of WORKSHEET II of Ref. 4 ; similarly, $\{\phi\}$ may be obtained from COLUMNS 205, 207, ... 217 . We have calculated the elements of $[\mathscr{S}]$ numerically to within ± 1 in the fourth significant figure and tabulated the results in Tables 6 - 9 for $\lambda = 0.25, 0.5, 0.75, 1.0$ and $i,j = 0\ ,\ \ldots\ 6$. The $[\mathscr{S}]\{a\}$ vector has also been calculated and is included in Table 1 for convenience.

The zero incidence contribution to the pressure coefficient may also be written in similar form, consisting of the two-dimensional part $\pm C(\bar{x})$ which gives a jump in pressure across the shroud plus a three-dimensional part which is continuous across the shroud as above, see Refs. 3 and 4 . Like $A(\bar{x})$, $C(\bar{x})$ may be written as $\{\varphi\}^T\{c\}$ where $\{c\}$ is a column vector of the Glauert coefficients for the vortex distribution on the given ducted propeller at zero incidence.

2.4 Shroud Forces and Moments

With the pressure coefficient in hand, the gross forces and moments for the shroud can be determined. Here we will limit ourselves for simplicity to the first-order quantities, namely the lift and its associated pitching moment. By symmetry about the xz-plane, there is no side force or yawing moment.

For first-order quantities, we need only the net loading $c_{p]} \equiv (c_p^- - c_p^+)$, positive radially outward. Eq. (27) gives

$$c_{p]} = -2\{\varphi\}^T\{c\} - 2\alpha\{\varphi\}^T\{a\}\sin\theta \tag{30}$$

which has the same chordwise variation as $c_{p]}$ for a two-dimensional airfoil. Therefore, the resulting elemental radial force and moment about the leading

edge on the strip $R\,d\theta$ by c follow immediately from thin airfoil theory. Resolving these as necessary and then integrating on θ, we find

$$c_{\ell} \equiv \frac{\ell}{\frac{1}{2}\rho U^2 \pi R^2} = -\pi\lambda(2a_0 + a_1)\alpha \tag{31}$$

$$c_{m} \equiv \frac{m}{\frac{1}{2}\rho U^2 \pi R^3} = \frac{\pi\lambda^2}{2}(2a_0 + 2a_1 - a_2)\alpha \tag{32}$$

where ℓ is the total lift on the shroud and m is the total pitching moment, positive nose-up, about an axis parallel to the y-axis and through the leading edge.

As we would expect, c_{ℓ} and c_{m} are the same as for the inclined duct alone. We hasten to point out, however, that Eq. (32) is correct only to first order. Practically, there are second-order terms due to the axial forces on the shroud which can give substantial contributions in addition, cf. Kriebel[13].

2.5 Propeller Forces and Moments

According to the superposition model the unsteady loading on the propeller is zero. Consequently, the only forces and moments we have are the usual thrust and torque as found in the case of zero incidence, see Ref. 4 .

{a}

ν \ λ	0.25	0.50	0.75	1.00
0	-1.4133	-1.0977	-0.9139	-0.7955
1	0.0985	0.2387	0.3456	0.4154
2	0.0040	0.0180	0.0409	0.0686
3	-0.0003	-0.0015	-0.0021	-0.0001
4	0.0000	-0.0003	-0.0012	-0.0024
5	0.0000	0.0000	-0.0001	-0.0005
6	0.0000	0.0000	0.0000	0.0000

$[\mathscr{P}]\{a\}$

ν \ λ	0.25	0.50	0.75	1.00
0	-0.2125	-0.1746	-0.1356	-0.1099
1	0.1627	0.2161	0.2246	0.2159
2	0.0089	0.0349	0.0636	0.0866
3	0.0006	0.0041	0.0114	0.0212
4	0.0000	0.0000	0.0006	0.0024
5	0.0000	0.0000	0.0000	0.0000
6	0.0000	0.0000	0.0000	-0.0001

TABLE 1

{a} AND $[\mathscr{P}]\{a\}$ VECTORS FOR SUPERPOSITION SOLUTION

1.4133	-0.2675	-0.0256	0.0004	0.0001	0.0000	0.0000
-0.0985	1.9462	0.0018	0.0028	0.0000	0.0000	0.0000
-0.0040	0.0008	1.9965	0.0000	0.0007	0.0000	0.0000
0.0003	0.0009	0.0000	1.9989	0.0000	0.0003	0.0000
0.0000	0.0000	0.0004	0.0000	1.9995	0.0000	0.0002
0.0000	0.0000	0.0000	0.0002	0.0000	1.9997	0.0000
0.0000	0.0000	0.0000	0.0000	0.0001	0.0000	1.9998

TABLE 2

INVERSION MATRIX $[\mathcal{O}]$ FOR $\lambda = 0.25$

1.0977	-0.3811	-0.0574	-0.0032	0.0004	0.0001	0.0000
-0.2387	1.8508	0.0147	0.0156	-0.0001	-0.0003	0.0000
-0.0186	0.0062	1.9812	0.0001	0.0036	0.0000	-0.0001
0.0015	0.0044	-0.0001	1.9949	0.0000	0.0005	0.0000
0.0003	-0.0001	0.0018	0.0000	1.9976	0.0000	0.0009
0.0000	-0.0001	0.0000	0.0009	0.0000	1.9986	0.0000
0.0000	0.0000	0.0000	0.0000	0.0006	0.0000	1.9991

TABLE 3

INVERSION MATRIX $[\mathcal{O}]$ FOR $\lambda = 0.50$

0.9139	-0.4268	-0.1072	-0.0101	0.0006	0.0003	0.0000
-0.3456	1.7469	0.0405	0.0412	-0.0002	-0.0012	0.0000
-0.0409	0.0191	1.9497	0.0005	0.0106	0.0000	-0.0004
0.0021	0.0115	-0.0002	1.9858	0.0000	0.0041	0.0000
0.0012	-0.0006	0.0052	0.0000	1.9939	0.0000	0.0022
0.0001	-0.0003	0.0000	0.0025	0.0000	1.9966	0.0000
0.0000	0.0000	-0.0001	0.0000	0.0003	0.0000	1.9990

TABLE 4

INVERSION MATRIX $[\mathcal{O}]$ FOR $\lambda = 0.75$

0.7955	-0.4418	-0.1406	-0.0206	-0.0002	0.0007	0.0002
-0.4154	1.6448	0.0734	0.0767	0.0001	-0.0025	-0.0001
-0.0686	0.0381	1.9040	0.0018	0.0230	-0.0001	-0.0011
0.0001	0.0219	0.0000	1.9696	0.0000	0.0089	0.0000
0.0024	-0.0013	0.0111	-0.0001	1.9872	0.0000	0.0044
0.0005	-0.0007	-0.0001	0.0053	0.0000	1.9932	0.0000
0.0000	0.0000	0003	0.0000	0.0030	0.0000	1.9957

TABLE 5

INVERSION MATRIX $[\mathcal{O}]$ FOR $\lambda = 1.00$

0.1557	0.0768	0	0.0011	0	0.0000	0
-0.1153	0	-0.0575	0	-0.0002	0	0.0000
-0.0043	0.0287	0	-0.0309	0	0.0000	0
-0.0004	0	0.0206	0	-0.0208	0	0.0000
0.0000	0.0000	0	0.0157	0	-0.0158	0
0.0000	0	0.0000	0	0.0125	0	-0.0125
0.0000	0.0000	0	-0.0002	0	0.0106	0

TABLE 6

$[\mathcal{G}']$ MATRIX FOR $\lambda = 0.25$

0.1772	0.0833	0	0.0053	0	0.0000	0
-0.1985	0	-0.0977	0	-0.0016	0	0.0000
-0.0211	0.0489	0	-0.0590	0	-0.0004	0
-0.0031	0	0.0393	0	-0.0408	0	-0.0001
0.0000	0.0004	0	0.0306	0	-0.0310	0
0.0000	0	0.0001	0	0.0248	0	-0.0249
0.0000	0.0000	0	0.0000	0	0.0208	0

TABLE 7

$[\mathcal{G}]$ MATRIX FOR $\lambda = 0.50$

0.1775	0.0771	0	0.0116	0	0.0001	0
-0.2512	0	-0.1206	0	-0.0050	0	0.0000
-0.0466	0.0603	0	-0.0822	0	-0.0014	0
-0.0099	0	0.0548	0	-0.0593	0	-0.0005
-0.0003	0.0012	0	0.0444	0	-0.0456	0
0.0000	0	0.0005	0	0.0365	0	-0.0370
0.0000	0.0000	0	0.0002	0	0.0308	0

TABLE 8

$[\mathscr{P}]$ MATRIX FOR $\lambda = 0.75$

0.1737	0.0682	0	0.0183	0	0.0004	0
-0.2827	0	-0.1310	0	-0.0104	0	0.0000
-0.0747	0.0655	0	-0.0995	0	-0.0034	0
-0.0207	0	0.0663	0	-0.0754	0	-0.0013
-0.0016	0.0026	0	0.0565	0	-0.0593	0
0.0000	0	0.0013	0	0.0475	0	-0.0488
0.0001	0.0000	0	0.0006	0	0.0404	0

TABLE 9

$[\mathscr{P}]$ MATRIX FOR $\lambda = 1.00$

CHAPTER THREE

INCLUSION OF SHROUD-PROPELLER COUPLING

3.1 The "Interaction Model"

Although the simple superposition hypothesis appears to be reasonable on physical grounds, it is not easily justified by the usual order of magnitude type reasoning. Therefore we will investigate the effect of the shroud-propeller coupling, manifested by the presence of $\mathscr{F}$ and $\mathscr{G}$ in the full integral equations, Eqs. (17) and (18) .

The only way this can be carried out practically is by an iteration procedure. That is, with A and B ($\equiv 0$) given by the superposition model as a first approximation, we calculate the corresponding θ-variation in inflow, or periodic gust, seen by each blade element as the propeller rotates. We then solve the associated unsteady propeller problem for $\hat{\Gamma}_\ell$. With $\hat{\Gamma}_\ell$, $\mathscr{F}$ and $\mathscr{G}$ follow and Eqs. (17) and (18) become equivalent to the equations of an inclined duct with non-axisymmetric camber. Consequently, these equations can be inverted in the same fashion and so, a second approximation found to A and B . The procedure may in turn be repeated successively.

Since $\mathscr{F}$ and $\mathscr{G}$ turn out to be fairly small compared to α , we limit the calculations for the present purposes to the second approximation. In addition, we assume $\hat{\Gamma}_\ell$ is uniform over the blade and determine the amplitude and phase of $\hat{\Gamma}_\ell$ by applying classical unsteady two-dimensional strip theory at a representative radius.

3.2 Determination of Unsteady Inflow and Propeller Circulation

We fix ourselves for the moment to the ℓth blade at the nominal point (x_p, r, θ_ℓ) , where

$$\theta_\ell \equiv -\Omega t + 2\pi\ell/N \tag{33}$$

so that the 0th blade coincides with the direction of the y-axis at $t = 0$. With $\cos\alpha \approx 1$, then the blade element centered about this point sees an effective free stream

$$\mathscr{U} \equiv \sqrt{U^2 + \Omega^2 r^2} \tag{34}$$

along the local helix angle, together with unsteady axial and tangential components of inflow.

Within our approximations, the unsteady axial component is due to the shroud

bound vortices and the unsteady tangential component, to the incidence crossflow and the shroud trailing vortices. We resolve these components parallel and perpendicular to $\mathscr{U}$. The effect of the parallel or surging component is small and may be neglected. For the perpendicular or unsteady downwash component, we find

$$w = u_{\gamma_1} \frac{\Omega r}{\mathscr{U}} - \left(U\alpha \cos\theta_\ell + w_{\gamma_1'} \right) \frac{U}{\mathscr{U}} \tag{35}$$

where w is taken positive if directed "downward". Analogous to Eq. (5), it can be shown that the axial velocity induced by the bound vortices of the duct loading $\gamma_1 = UA \sin\theta$ is proportional to $U\alpha \sin\theta$, and that the tangential velocity induced by the associated trailing vortices is proportional to $U\alpha \cos\theta$. Setting $\theta = \theta_\ell$ and combining the latter term with the crossflow term, we can rewrite Eq. (35) as

$$w = -\frac{\alpha U^2}{\mathscr{U}} \left(\frac{\bar{r}}{J\mu} \Pi_u \sin\theta_\ell + \Pi_w \cos\theta_\ell \right) \tag{36}$$

where $J \equiv U/\Omega R_p$ is the advance ratio of the propeller, $\mu \equiv R_p/R$ and

$$\Pi_u \equiv \frac{1}{4\pi \bar{r}^{3/2}} \int_{-\lambda}^{\lambda} \left[2Q'_{\frac{1}{2}} - \bar{r}Q'_{-\frac{1}{2}} - \bar{r}Q'_{\frac{1}{2}} \right] \frac{A}{\alpha} \, d\bar{x}_v \tag{37}$$

$$\Pi_w \equiv 1 + \frac{1}{4} \int_{-\lambda}^{\lambda} \left\{ 1 - \frac{1+\bar{r}^2}{2\bar{r}^2} \Lambda_o - \frac{\Delta\bar{x}_v}{2\pi \bar{r}^{5/2}} \left[2\bar{r}Q_{\frac{1}{2}} + (1-\bar{r}^2)Q_{-\frac{1}{2}} \right] \right\} \frac{A}{\alpha} \, d\bar{x}_v \tag{38}$$

with $A(\bar{x}_v)/\alpha$ given by Eqs. (21) and Table 1. The argument β and modulus κ of the Heuman lambda function $\Lambda_o(\beta,\kappa)$ are

$$\beta = \sin^{-1} \sqrt{\frac{(\Delta\bar{x}_v)^2}{(\Delta\bar{x}_v)^2 + (1-\bar{r})^2}} \quad , \quad \kappa = \sqrt{\frac{4\bar{r}}{(\Delta\bar{x}_v)^2 + (1+\bar{r})^2}} \tag{39}$$

and the argument of the Legendre functions is

$$\omega = 1 + [(\Delta\bar{x}_v)^2 + (1-\bar{r})^2] / 2\bar{r} \tag{40}$$

For $\bar{r} = 0.7$, the constants Π_u, Π_w have been evaluated by numerical integration for several values of λ and x_p/c to an accuracy of ± 0.0001, and are tabulated in Table 10.

Π_u

λ \ x_p/c	-0.25	-0.125	0.0	0.125	0.25
0.25	0.5506	0.5201	0.4696	0.4088	0.3449
0.50	0.6182	0.5113	0.4021	0.3046	0.2207
0.75	0.5445	0.3938	0.2753	0.1867	0.1200
1.00	0.4488	0.2863	0.1789	0.1090	0.0624

Π_w

λ \ x_p/c	-0.25	-0.125	0.0	0.125	0.25
0.25	0.8195	0.8568	0.8985	0.9413	0.9830
0.50	0.8418	0.9298	1.0119	1.0846	1.1474
0.75	0.9128	1.0327	1.1308	1.2090	1.2708
1.00	0.9894	1.1248	1.2248	1.2978	1.3511

TABLE 10

INDUCED VELOCITY FACTORS Π_u , Π_w FOR $\bar{r} = 0.7$

The chordwise point we chose on the blade element was arbitrary. If we had taken another point at a distance ξ further along the chord in the $\mathscr{U}$-direction, α would still be given by Eq. (36) but with θ_ℓ replaced by θ_ℓ plus the increment $\xi\Omega/\mathscr{U}$. Recalling Eq. (33) then, we see this resulting downwash is equivalent to the sinusoidal gust problem solved by N. Kemp[15] and others. Taking d as the chord length of the element and adapting his solution, we get

$$\hat{\Gamma}_\ell = \alpha U d \sigma \cos(\theta_\ell - \vartheta) \tag{41}$$

with the amplitude factor σ and phase angle ϑ given by

$$\sigma = \pi \frac{U}{\mathscr{U}} \sqrt{\left[\Pi_w a^r - \frac{\bar{r}}{J\mu}\Pi_u a^i\right]^2 + \left[\Pi_w a^i + \frac{\bar{r}}{J\mu}\Pi_u a^r\right]^2} \tag{42}$$

$$\vartheta = \tan^{-1}\left[\frac{J\mu\Pi_w a^i + \bar{r}\Pi_u a^r}{J\mu\Pi_w a^r - \bar{r}\Pi_u a^i}\right] \tag{43}$$

The factors a^r and a^i depend only on the reduced frequency

$$k \equiv \Omega d/2\mathscr{U} \tag{44}$$

and in terms of the Bessel and Hankel functions are defined by

$$a \equiv a^r + ia^i \equiv (2e^{-ik}/\pi k)\frac{J_1 + iJ_0}{H_1^{(2)} + iH_0^{(2)}} \tag{45}$$

These are tabulated in Table 11 .

3.3 Calculation of Shroud-Propeller Coupling

For uniform $\hat{\Gamma}_\ell$, we are concerned only with concentrated helical vortices trailing from each of the N blade tips. If τ represents the parametric time for a vortex element to convect downstream, its strength at any point is $\alpha U d\sigma \cos(\theta_\ell - \vartheta + \Omega\tau)$ and varies periodically along the length of the helix.

The total radial wash, steady and unsteady, induced on the shroud by these vortices may then be expressed according to the Biot-Savart law in the same fashion as for a helical vortex of constant strength except for the above cosine dependence which now appears in the τ-integration. To obtain the steady part, we integrate in turn with respect to Ωt over the period 2π and divide by 2π . If the order of integration is inverted, the Ωt-integration may be performed explicitly in terms of Legendre functions. The result is independent of the blade index ℓ , so that the summation over the blade number merely produces a factor N . It may therefore be shown that

$$v_{\hat{r}'} = -\frac{\alpha U \mu^{\frac{1}{2}} N \sigma d}{8\pi^2 R_p}\left\{\cos\Delta\theta\int_0^\infty \Delta\bar{x}_{p\tau}(Q'_{\frac{1}{2}} + Q'_{-\frac{1}{2}})d\bar{\tau} + J\mu\sin\Delta\theta\int_0^\infty (Q'_{\frac{1}{2}} - Q'_{-\frac{1}{2}})d\bar{\tau}\right\} \tag{46}$$

with $\Delta\bar{x}_{p\tau} \equiv (\bar{x} - \bar{x}_p - J\mu\bar{\tau})$, $\bar{\tau} \equiv \Omega\tau$, $\Delta\theta \equiv (\theta - \vartheta)$ and the argument of the Q's

k	a^r	a^i	b^r	b^i
0.0000	1.0000	0.0000	1.0000	0.0000
0.0400	0.9153	-0.1697	0.9240	-0.1145
0.0800	0.8273	-0.2553	0.8526	-0.1546
0.1200	0.7484	-0.3065	0.7926	-0.1678
0.1600	0.6796	-0.3382	0.7429	-0.1675
0.2000	0.6199	-0.3581	0.7016	-0.1596
0.2400	0.5677	-0.3705	0.6667	-0.1476
0.2800	0.5218	-0.3779	0.6369	-0.1333
0.3200	0.4811	-0.3820	0.6110	-0.1177
0.3600	0.4447	-0.3836	0.5882	-0.1014
0.4000	0.4119	-0.3836	0.5679	-0.0849
0.4400	0.3821	-0.3823	0.5495	-0.0684
0.4800	0.3548	-0.3801	0.5326	-0.0521
0.5200	0.3297	-0.3772	0.5169	-0.0360
0.6000	0.2849	-0.3699	0.4884	-0.0049
0.7000	0.2368	-0.3590	0.4561	0.0318
0.8000	0.1954	-0.3467	0.4260	0.0659
0.9000	0.1591	-0.3335	0.3971	0.0972
1.0000	0.1269	-0.3196	0.3686	0.1259

TABLE 11

UNSTEADY AIRFOIL THEORY COEFFICIENTS a(k) AND b(k)

is given by

$$\omega \equiv 1 + [(\Delta\bar{x}_{p\tau})^2 + (1-\mu)^2]/2\mu \qquad (47)$$

The first integral is an exact differential and can be evaluated immediately. Integration of the second integral, however, is quite difficult. After considerable manipulation, we can find an approximate result. The approximation is in the sense that μ is close to unity, which is true in practice. Thus, we have

$$\mathscr{F} \approx -\frac{\alpha\mu^{\frac{1}{2}}N\sigma d}{8\pi^2 R_p}\left\{\frac{1}{J}(Q_{\frac{1}{2}}+Q_{-\frac{1}{2}})\sin\vartheta + \mu^{\frac{3}{2}}[\pi(2-\mu)+\Delta\bar{x}_p(Q_{\frac{1}{2}}+Q_{-\frac{1}{2}})]\cos\vartheta\right\} \qquad (48)$$

where ω is now given by Eq. (47) with $\bar{\tau} = 0$. The function $\mathscr{G}$ is identical to $\mathscr{F}$, with $\sin\vartheta$ and $\cos\vartheta$ replaced by $\cos\vartheta$ and $-\sin\vartheta$ respectively.

Before evaluating $\mathscr{F}$ and $\mathscr{G}$ one point should be made regarding their form. Notice that both terms are proportional to N. It would therefore seem that for a given value of the steady part of the propeller thrust, they could be made arbitrarily large — and hence also the corresponding shroud loading — by increasing the blade number. Actually, as N becomes large, the effect of blade interference would come into play and decrease the amplitude of the unsteady propeller circulation.

To illustrate the quantitative and qualitative importance of the shroud-propeller coupling, consider the typical set of parameters $N = 3$, $\mu = 0.95$,

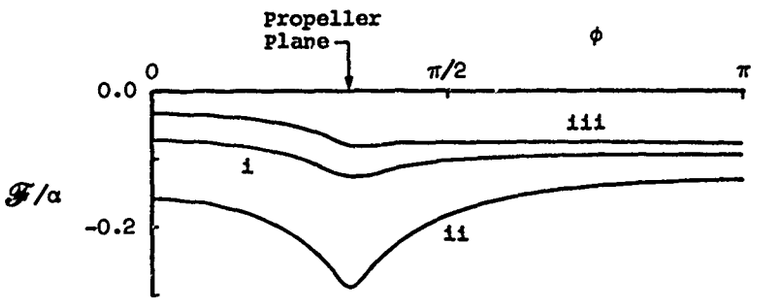

FIGURE 4

$d/R_p = 0.2$, $x_p/c = -0.25$ for three cases: (i) $\lambda = 0.5$, $J = 0.5$; (ii) $\lambda = 0.5$, $J = 0.25$; (iii) $\lambda = 1.0$, $J = 0.5$. We have calculated $\mathscr{F}$ and $\mathscr{G}$

and plotted them against the Glauert variable in Figs. 4 and 5 .

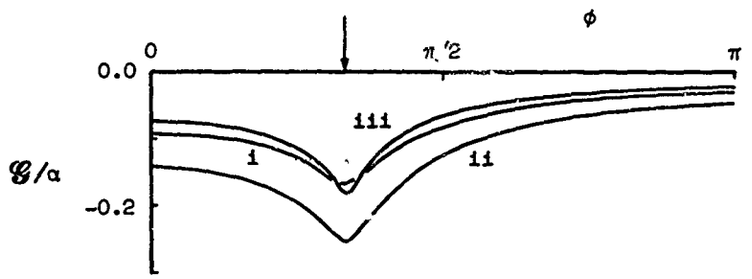

FIGURE 5

Since their importance is determined by their magnitude relative to unity, we see that the shroud-propeller coupling is in fact large enough to account for a significant improvement over the simple superposition model, but not large enough to discredit the superposition model as a reasonable first approximation.

Parametrically, comparison of these cases indicates an increase in the magnitude of the coupling terms as J decreases and/or λ increases.

3.4 The Interaction Solution

The second approximation or interaction solution, i.e. including the effect of the shroud-propeller coupling, may be constructed easily using the inclined-duct results or Weissinger's general formulation[6]. We take

$$A = \alpha \left[a_0 \cot \frac{\phi}{2} + \sum_{\nu=1}^{\infty} a_\nu \sin \nu\phi \right] \tag{49}$$

$$B = \alpha \left[b_0 \cot \frac{\phi}{2} + \sum_{\nu=1}^{\infty} b_\nu \sin \nu\phi \right] \tag{50}$$

and expand the coupling terms as

$$\mathscr{F}/\alpha \equiv f_0 - \sum_{\nu=1}^{\infty} f_\nu \cos \nu\phi \tag{51}$$

$$\mathcal{G}/\alpha \equiv \mathcal{g}_0 - \sum_{\nu=1}^{\infty} \mathcal{g}_\nu \cos \nu\phi \tag{52}$$

Then, it is not difficult to show that, analogous to Eq. (23) ,

$$\{a\} = - [\mathcal{O}] \{ (1+\mathcal{f}_0) , \mathcal{f}_1 , \mathcal{f}_2 \cdots \}^T \tag{53}$$

$$\{b\} = - [\mathcal{O}] \{ \mathcal{g}_0 , \mathcal{g}_1 , \mathcal{g}_2 , \cdots \}^T \tag{54}$$

where the $\mathcal{f}_\nu$'s and $\mathcal{g}_\nu$'s must be computed by numerical Fourier analysis.

3.5 Shroud Surface Pressures

Direct extension of the matrix form for the shroud surface pressures from Eq. (27) yields,

$$c_p = c_{p_0} + \alpha(\pm\{\varphi\}^T - \{\phi\}^T[\mathcal{S}]) (\{a\}\sin\theta + \{b\}\cos\theta) \tag{55}$$

where we recall that the values of $[\mathcal{S}]$ have already been presented in Tables 6-9 .

3.6 Shroud Forces and Moments

Consistent with the superposition model, we will consider only first-order contributions to the forces and moments.

If we write down the net loading c_p] , we have three terms, i.e. an axisymmetric term, a $\sin\theta$ term and a $\cos\theta$ term. The axisymmetric term is identically the same as for the superposition model and again does not contribute to any gross quantity. The $\sin\theta$ term is also the same in form and gives a lift and associated pitching moment as expressed by Eqs. (31) and (32) , only the a_ν's of Eq. (23) are replaced by the a_ν's of Eq. (53) . The $\cos\theta$ term is completely new and has not appeared in other analyses. It is symmetric about the xy-plane and causes a side force $\mathcal{s}$ and yawing moment $\mathcal{m}$ which by analogy with the lift force and pitching moment are,

$$C_{\mathcal{s}} \equiv \frac{\mathcal{s}}{\frac{1}{2}\rho U^2 \pi R^2} = - \pi\lambda(2a_0 + a_1)\alpha \tag{56}$$

$$C_{\mathcal{m}} \equiv \frac{\mathcal{m}}{\frac{1}{2}\rho U^2 \pi R^3} = - \frac{\pi\lambda^2}{2} (2b_0 + 2b_1 - b_2)\alpha \tag{57}$$

The side force is positive in the positive y-direction and the yawing moment, taken about an axis parallel to the z-axis and through the leading edge, is positive in the nose-right direction.

3.7 Propeller Forces and Moments

For the superposition model, we had only the usual thrust and torque on the propeller. For the interaction model, though, we must expect additional forces and moments corresponding to $v_{A'}$.

To compute these quantities, the local unsteady "lift" is needed for each blade element. From Kemp[15] again, this is given by the so-called Kutta-Joukowski lift, times the factor $e^{ik}/[J_0(k) - iJ_1(k)]$. If the latter is combined with the circulation, however, the resulting unsteady lift per unit length may be reduced to the same form $\rho \mathcal{U} \hat{\Gamma}_\ell$ with $a^{r,i}$ in σ and ϑ of Eqs. (42) and (43) replaced by $b^{r,i}$ where

$$b \equiv b^r + ib^i \equiv a \cdot \frac{e^{ik}}{J_0 - iJ_1} \tag{58}$$

The quantity $b(k)$ is identical to "$S(\omega)$" tabulated by Kemp[15] and partially reproduced here for convenience back in Table 11 . Of course, $b \to a$ as $k \to 0$.

If we resolve the above incremental lift into its y- and z-components, integrate over the blade radius, and sum over the N blades, we find that the associated total propeller lift and side force are

$$L + \hat{L} = \alpha\rho U^2 R_p d\sigma_b \sum_{\ell=0}^{N-1} \cos(\theta_\ell - \vartheta_b) \cos\theta_\ell \tag{59}$$

$$S + \hat{S} = -\alpha\rho U^2 R_p d\sigma_b \sum_{\ell=0}^{N-1} \cos(\theta_\ell - \vartheta_b) \sin\theta_\ell \tag{60}$$

where $\sigma_b \equiv \sigma(b^{r,i})$ and $\vartheta_b \equiv \vartheta(b^{r,i})$. Expressing the sines and cosines in exponential form, the steady portions of these summations may be evaluated explicitly as $\frac{1}{2} N \cos\vartheta_b$ and $\frac{1}{2} N \sin\vartheta_b$ respectively. It follows that the steady lift L and side force S are

$$C_L \equiv \frac{L}{\frac{1}{2}\rho U^2 \pi R^2} = \frac{\alpha\mu^2 N\sigma_b d}{\pi R_p} \cos\vartheta_b \tag{61}$$

$$C_S \equiv \frac{S}{\frac{1}{2}\rho U^2 \pi R^2} = -\frac{\alpha \mu^2 N \sigma_b d}{\pi R_p} \sin \vartheta_b \tag{62}$$

The resultant force vector is oriented at the angle $\theta = (\vartheta_b + \pi/2)$. Similarly, we can obtain the pitching moment M and yawing moment N as

$$C_M \equiv \frac{M}{\frac{1}{2}\rho U^2 \pi R^3} = -\frac{\alpha \mu^3 N \sigma_b d}{3\pi J R_p} \sin \vartheta_b \tag{63}$$

$$C_N \equiv \frac{N}{\frac{1}{2}\rho U^2 \pi R^3} = \frac{\alpha \mu^3 N \sigma_b d}{3\pi J R_p} \cos \vartheta_b \tag{64}$$

with the nose-up and nose-right directions taken positive as for the shroud. Again the resultant moment vector is oriented at the angle $\theta = (\vartheta_b + \pi/2)$.

These additional forces and moments are closely related to those obtained by programmed blade pitch variation as studied by W.P.A. Joosen et al[16] in connection with the control of tandem-propeller submarines.

CHAPTER FOUR

NUMERICAL RESULTS AND COMPARISON WITH EXPERIMENT

4.1 Cases Chosen

For comparison with experiment, we have chosen Cases "2", "3" and "4" of Ref. 17 where

Case	λ	μ	J
"2"	0.345	0.970	0.355
"3"	0.500	0.956	0.344
"4"	0.724	0.936	0.406

with $N = 3$, $x_p/c = -0.219$ and $d/R_p = 0.213$ in each case. The values of J and d/R_p, not given therein, were obtained by private communication with the author.

4.2 Theoretical Results

Let us outline the calculations for one case, say Case "3". For the superposition model, the {a} vector is given directly up to $\nu = 6$ by Table 1. The surface pressure coefficient is found then from Eq. (27), and the lift and moment from Eqs. (31) and (32).

For the solution according to the interaction model, we first compute the reduced frequency $k = 0.132$ from Eq. (44) and hence obtain $a^r = 0.727$ and $a^i = -0.318$ from Table 11. From Table 10, the inflow factors are $\Pi_u = 0.592$ and $\Pi_w = 0.864$. Eqs. (42) and (43) then give the amplitude factor $\sigma = 1.678$ and phase angle $\vartheta = 31.9°$. With these, $\mathscr{F}/\alpha$ and $\mathscr{G}/\alpha$ may be calculated over the shroud chord from Eq. (48), and $\mathscr{f}_\nu = -0.1277, 0.0095, -0.0224, -0.0184, -0.0020, 0.0081, 0.0066$ and $\mathscr{g}_\nu = -0.1123, 0.0575, -0.0277, -0.0313, -0.0059, 0.0120, 0.0111$ obtained by numerical Fourier analysis, see Eqs. (51) and (52). The Glauert coefficient vectors {a} and {b} follow from Eqs. (53) and (54), and hence the angle of attack portion of the net surface pressure coefficient from Eq. (55). With {a} and {b}, we may then evaluate the gross duct quantities easily from Eqs. (31), (32), (56) and (57). For the propeller, however, we must first determine $\sigma_b = 1.624$ and $\vartheta_b = 43.4°$ from Eqs. (42) and (43), with a^r and a^i replaced by $b^r = 0.778$ and $b^i = -0.168$ from Table 11. In turn, the steady forces and moments on the propeller, which arise due to the unsteady portion of the blade loading, are found from Eqs. (61) - (64).

All of these results for the interaction model are compared with the results of the superposition model in the following tables and Fig. 6 . The overall effect of the shroud-propeller interaction may be seen clearly. From

	Superposition Model		Interaction Model	
v	(a)	(b)	(a)	(b)
0	-1.0977	0	-0.9555	0.1432
1	0.2387	0	0.1912	-0.1323
2	0.0180	0	0.0601	0.0526
3	-0.0015	0	0.0354	0.0623
4	0.0003	0	0.0038	0.0119
5	0.0000	0	-0.0161	-0.0240
6	0.0000	0	-0.0132	-0.0222

the two values of $dC_\ell/d\alpha$, we find that it causes a reduction of about 10% in the shroud lift or, equivalently, in the "effective" incidence. This, however, is approximately compensated for by the introduction of a propeller lift, see $dC_L/d\alpha$, so that the combined lift of the shroud and propeller remains about the same. This compensatory effect is not present, though, in the case of the side force generated by the interaction. There the shroud and propeller side forces are additive and produce a resultant force equal in magnitude to about 15% of the lift, see $dC_\delta/d\alpha$ and $dC_S/d\alpha$. Regarding the moments, we see that the interaction increases the pitching moment by about 20% and also introduces a yawing moment about 30% as big.

Quantity	Superposition Model	Interaction Model
$dC_\ell/d\alpha$	3.074	2.701
$dC_\delta/d\alpha$	0	-0.242
$dC_m/d\alpha$	-0.682	-0.624
$dC_n/d\alpha$	0	0.013
$dC_L/d\alpha$	0	0.219
$dC_S/d\alpha$	0	-0.207
$dC_M/d\alpha$	0	-0.192
$dC_N/d\alpha$	0	0.203

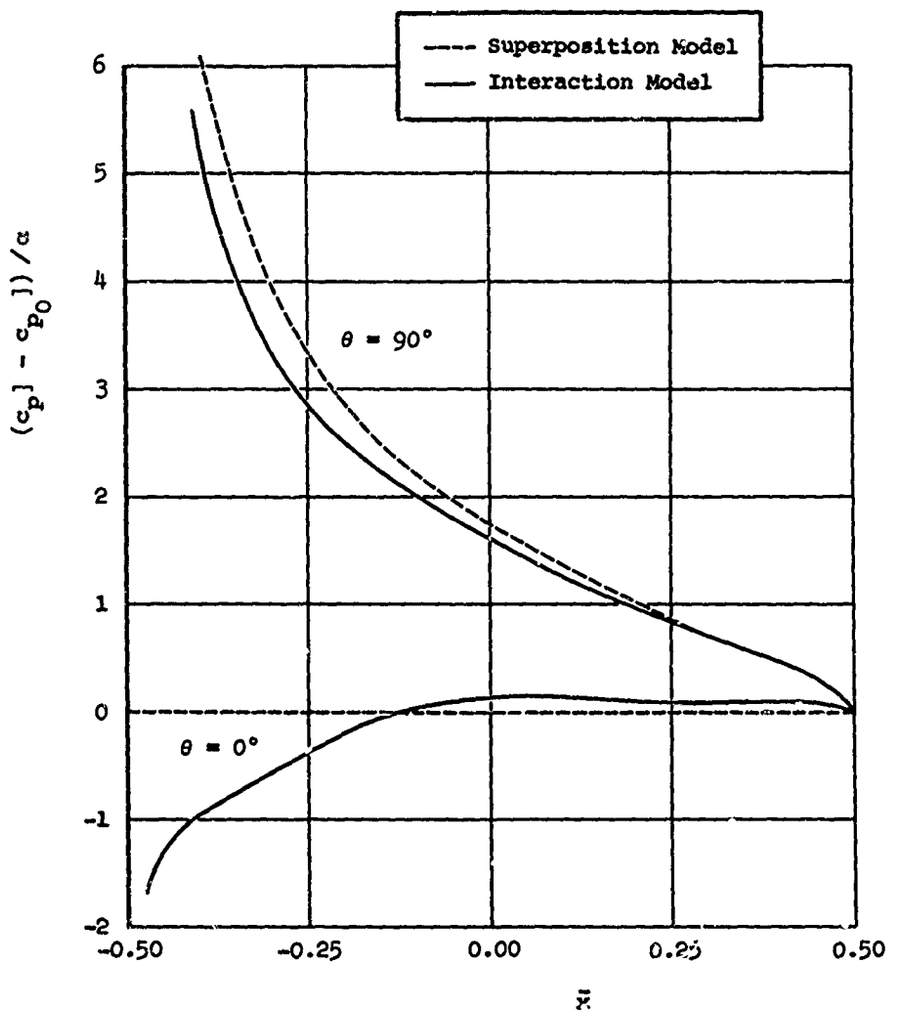

FIGURE 6

ANGLE OF ATTACK CONTRIBUTION TO NIT SHROUD PRESSURE COEFFICIENT COMPARISON OF MODELS FOR CASE "3"

We have omitted the corresponding calculations for Cases "2" and "4" for brevity. They are entirely similar to Case "3", both quantitatively and qualitatively.

4.3 Comparison with Experiment

The total lift $\mathscr{L}$ on the ducted propeller in general is equal to the sum of the duct lift, the propeller lift and the component of the total thrust $\mathscr{T}$ normal to the stream. Putting this in coefficient form and taking $d(\ )/d\alpha$ of the result gives

$$\frac{d}{d\alpha} c_{\mathscr{L}} - c_{\mathscr{T}} = \frac{d}{d\alpha} c_{\ell} + \frac{d}{d\alpha} c_{L} \tag{65}$$

Experimental values for the terms on the left hand side (LHS) are given in Ref. 17 . For comparison, the terms on the right hand side (RHS) have been computed as outlined. These results, based upon the interaction model, are presented in the following table.

Case	$\frac{d}{d\alpha} c_{\mathscr{L}}$	$c_{\mathscr{T}}$	$\frac{d}{d\alpha} c_{\ell}$	$\frac{d}{d\alpha} c_{L}$	LHS	RHS
"2"	3.04	0.2	2.30	0.23	2.84	2.53
"3"	3.34	0.2	2.70	0.22	3.14	2.92
"4"	3.61	0.2	3.11	0.23	3.41	3.34

The corresponding values of the RHS for the superposition model are 2.57, 3.07 and 3.49, which differ very little from the values predicted by the interaction model. Where the two models do differ significantly though, is in the prediction of the side force and the breakdown of the total lift between the duct and propeller. Unfortunately, these new forces and moments are not reported in Ref. 17 , nor elsewhere as far as we know, and must await further tests for substantiation.

CONCLUSIONS

A theory has been developed for the steady portion of the aerodynamic loading on a ducted propeller in forward flight at angle of attack. In particular:

We have shown that as a first approximation the ducted propeller at angle of attack may, without a priori assumption, be regarded as the superposition of the given ducted propeller at zero incidence plus a cylindrical duct of the same aspect ratio but zero thickness and camber at the given incidence. Formulas and tables are presented for the convenient calculation of the cylindrical-duct portion, the ducted propeller at zero incidence having been treated in previous reports.

This approximation has also been refined to include the effect of the cyclic variation of blade loading, due to the asymmetric flow through the propeller plane, and the associated interaction with the shroud. The results are reduced to a tractable form and provide an improvement over the superposition model that is significant, though not great enough to invalidate the superposition theory as a first approximation.

More important, the improved "interaction" model predicts a net side force not accounted for at all by the simple superposition model. It may be as great as 20% or more of the lift; approximately half on the propeller and half on the shroud. A decrease in shroud lift of around 10% is also predicted by the interaction model, although it is approximately balanced by a lift force on the propeller.

Comparison with tests shows good agreement for the values of total ducted propeller lift. Unfortunately, neither side forces nor propeller lift have been measured experimentally so that direct verification of the additional loads predicted by the interaction model is not possible at this time.

In the light of these new results, we recommend that certain aspects of the overall aerodynamic design of VTOL ducted-propeller aircraft be re-examined as well as the detailed mechanical design of the shroud and propeller components.

REFERENCES

1. Ordway, D. E., Sluyter, M. M., and Sonnerup, B. U. O., Three-Dimensional Theory of Ducted Propellers, THERM, Incorporated, TAR-TR 602, August 1960.

2. Ordway, D. E., and Greenberg, M. D., General Harmonic Solutions for the Ducted Propeller, THERM, Incorporated, TAR-TR 613, August 1961.

3. Hough, G. R., The Aerodynamic Loading on Streamlined Ducted Bodies, THERM, Incorporated, TAR-TR 625, December 1962. Also see Developments in Mechanics, Pergamon Press, pp. 340-357, 1965.

4. Kaskel, A. L., Ordway, D. E., Hough, G. R., and Ritter, A., A Detailed Numerical Evaluation of Shroud Performance for Finite-Bladed Ducted Propellers, THERM, Incorporated, TAR-TR 639, December 1963.

5. Greenberg, M. D., and Ordway, D. E., The Ducted Propeller in Static and Low-Speed Flight, Therm Advanced Research, Inc., TAR-TR 6407, October 1964.

6. Ribner, H., The Ring Airfoil in Nonaxial Flow, J. Aero. Sci., Vol. 14, No. 9, pp. 529-530, 1947.

7. Weissinger, J., Zur Aerodynamik des Ringflügels in inkompressibler Strömung, ZFW, Heft 3/4, pp. 141-150, March/April, 1956.

8. Weissinger, J., Finige Ergebnisse aus der Theorie des Ringflügels in inkompressibler Strömung, Advances in Aeronautical Sciences, Pergamon Press, Vol. 2, pp. 798-831, 1959.

9. Ladurner, O., Theoretical Investigation and Examination by Measuring Tests in What a Degree the Economy of Flying Vehicles is Influenced by Pre-Cambered Skeletons of Airfoils Closed in Themselves, Bureau Technique Zborowski, DA-91-508-EUC393, August 1959.

10. Fletcher, H. S., Experimental Investigation of Lift, Drag, and Pitching Moment of Five Annular Airfoils, NACA TN 4117, October 1957.

11. Ribner, H., Propellers in Yaw, NACA Report No. 820, 1945.

12. Miller, R. H., Rotor Blade Harmonic Airloading, IAS Paper No. 62-82, Presented at IAS 30th Annual Meeting, New York, New York, January 1962.

13. Kriebel, A. R., Theoretical Investigation of Static Coefficients, Stability Derivatives, and Interference for Ducted Propellers, Itek Corp., Vidya Report No. 112, March 1964.

14. Robinson, A., and Laurmann, J. A., Wing Theory, Cambridge University Press, 1956.

15. Kemp, N. H., On the Lift and Circulation of Airfoils in Some Unsteady Flow Problems, J. Aero. Sci., Vol. 19, No. 10, p. 713-714, 1952.

16. Joosen, W. P. A., van Manen, J. D., and van der Walle, F., Large Hub to Diameter Ratio Propellers With Programmed Blade Control, Proc. Fourth Symp. on Naval Hydrodynamics, Washington, U.S.A., 1962.

17. Johnson, A. E., Wind-Tunnel Investigation of the Effects of Thrust, Shroud Length, and Shroud Camber on the Static Stability Characteristics of Shrouded Propellers, David Taylor Model Basin, Aero. Rep. No. 1073, April 1964.

DISTRIBUTION LIST

CONTRACT Nonr 4357(00)

Chief, Bureau of Naval Weapons
(RAAD-3)
Department of the Navy
Washington, D. C. 20360 — 1

Chief, Bureau of Naval Weapons
(RAAD-332)
Department of the Navy
Washington, D. C. 20360 — 1

Chief, Bureau of Naval Weapons
(RA-4)
Department of the Navy
Washington, D. C. 20360 — 1

Chief, Bureau of Naval Weapons
(RAPP-22)
Department of the Navy
Washington, D. C. 20360 — 1

Chief, Bureau of Naval Weapons
(RRRE-4)
Department of the Navy
Washington, D. C. 20360 — 1

Commanding Officer and Director
David Taylor Model Basin
Aerodynamics Laboratory Library
Washington, D. C. 20007 — 1

Chief of Naval Research
Department of the Navy
Washington, D. C. 20360
Attn: Code 461 — 6

Chief of Naval Research
Department of the Navy
Washington, D. C. 20360
Attn: Code 438 — 1

Commanding Officer
Office of Naval Research Branch
Office
Box 39 F.P.O.
New York, New York 09510
Attn: CDR H. A. Smith — 2

Director
Naval Research Laboratory
Technical Information Office
Washington, D. C. 20390 — 6

Commander
U.S. Army Materiel Command
Department of the Army
Washington, D. C. 20315
Attn: AMCRD-RP-A — 1

Commanding Officer
U.S. Army Aviation Materiel
Laboratories
Fort Eustis, Virginia 23604
Attn: OSMFE-AM — 1
Research Reference Center — 1

U.S. Army Research Center
Physical Sciences Division
3045 Columbia Pike
Arlington, Virginia 20310
Attn: Mr. R. Ballard — 1

U.S. Army Research Office -
Durham
Box CM, Duke Station
Durham, North Carolina
Attn: Dr. S. Kumar — 1

Commanding Officer
Army Aero Activity (226-5)
Ames Research Center
Moffett Field, California
Attn: Technical Director — 1

U.S. Air Force (SREM)
Office of Scientific Research
Washington, D. C. 20333 — 1

Research and Technology Division
Wright-Patterson Air Force Base
Ohio 45433
Attn: AFFDL-FDV — 1

Research and Technology Division
Wright-Patterson Air Force Base
Ohio 45433
Attn: FDM 1

Defense Documentation Center
Headquarters, Cameron Station
Building No. 5
Alexandria, Virginia 22314 20

National Aeronautics and Space Administration
600 Independence Avenue, S.W.
Washington, D. C. 20546
Attn: Code RAP 1
RAA 1

National Aeronautics and Space Administration
Langley Research Center
Langley Station
Hampton, Virginia 23365
Attn: Mr. Donely 1

National Aeronautics and Space Administration
Ames Research Center
Moffett Field, California
Attn: Full Scale Research Division (Mr. Cook) 1

Library
American Institute of Aeronautics and Astronautics
1290 Avenue of the Americas
New York, New York 10019 1

Cornell Aeronautical Laboratory, Inc.
4455 Genesee Street
Buffalo, New York 14221
Attn: Mr. R. P. White, Jr. 1

Georgia Institute of Technology
Daniel Guggenheim School of Aerospace Engineering
Atlanta, Georgia 30332
Attn: Dr. R. B. Gray 1

Princeton University
Department of Aerospace and Mechanical Sciences
James Forrestal Research Center
Princeton, New Jersey
Attn: Prof. David C. Hazen 1

Naval Postgraduate School
Aeronautical Engineering Department
Monterey, California
Attn: Dr. R. Head 1

Syracuse University
Mechanical Engineering Department
Syracuse, New York
Attn: Dr. S. Eskinazi 1

University of Virginia
Aerospace Engineering Department
Charlottesville, Virginia
Attn: Dr. G. B. Matthews 1

Douglas Aircraft Company, Inc.
Aircraft Division
Long Beach, California
Attn: Mr. A. M. O. Smith, Supervisor, Aerodynamics Research Group 1

Therm Advanced Research, Inc.
100 Hudson Circle
Ithaca, New York
Attn: Dr. A. Ritter 1

Vidya Division
1450 Page Mill Road
Stanford Industrial Park
Palo Alto, California
Attn: Dr. J. N. Nielsen 1

Unclassified
Security Classification

DOCUMENT CONTROL DATA - R&D

(Security classification of title, body of abstract and indexing annotation must be entered when the overall report is classified)

1 ORIGINATING ACTIVITY *(Corporate author)*
Therm Advanced Research, Inc.
Ithaca, New York 14850

2a. REPORT SECURITY CLASSIFICATION
Unclassified

2b GROUP

3. REPORT TITLE
A THREE-DIMENSIONAL THEORY FOR THE DUCTED PROPELLER AT ANGLE OF ATTACK

4. DESCRIPTIVE NOTES *(Type of report and inclusive dates)*
Final Report

5. AUTHOR(S) *(Last name, first name, initial)*
Greenberg, M. D.
Ordway, D. E.
Lo, C. F.

6. REPORT DATE	7a. TOTAL NO. OF PAGES	7b. NO. OF REFS
December 1965	34	17

8a. CONTRACT OR GRANT NO.
Nonr-4357(00)
b. PROJECT NO.
NR 212-103
c.
d.

9a. ORIGINATOR'S REPORT NUMBER(S)
TAR-TR 6509

9b. OTHER REPORT NO(S) *(Any other numbers that may be assigned this report)*
None

10. AVAILABILITY/LIMITATION NOTICES
Qualified requesters may obtain copies of this report from DDC.

11. SUPPLEMENTARY NOTES
None

12. SPONSORING MILITARY ACTIVITY
Air Programs, Office of Naval Research, Washington, D. C.

13. ABSTRACT

An inviscid theory is developed for the steady aerodynamic loading on a ducted propeller in forward flight at angle of attack. As a first approximation, the problem is regarded as the superposition of the given ducted propeller at zero incidence and a cylindrical duct of the same aspect ratio but of zero thickness and camber at the given incidence. This approximation is then improved to include the cyclic variation of the blade loading. Not only are the normal force and pitching moment changed but also a finite side force and yawing moment, unknown heretofore, are found. Explicit formulas are given to carry out numerical calculations and a limited comparison with experimental results show good agreement.

DD FORM 1 JAN 64 1473

Unclassified
Security Classification

14. KEY WORDS	LINK A		LINK B		LINK C	
	ROLE	WT	ROLE	WT	ROLE	WT
VTOL Aircraft Design Ducted Propeller Theory Ring Wing Theory Unsteady Propeller Theory						

INSTRUCTIONS

1. ORIGINATING ACTIVITY: Enter the name and address of the contractor, subcontractor, grantee, Department of Defense activity or other organization *(corporate author)* issuing the report.

2a. REPORT SECURITY CLASSIFICATION: Enter the overall security classification of the report. Indicate whether "Restricted Data" is included. Marking is to be in accordance with appropriate security regulations.

2b. GROUP: Automatic downgrading is specified in DoD Directive 5200.10 and Armed Forces Industrial Manual. Enter the group number. Also, when applicable, show that optional markings have been used for Group 3 and Group 4 as authorized.

3. REPORT TITLE: Enter the complete report title in all capital letters. Titles in all cases should be unclassified. If a meaningful title cannot be selected without classification, show title classification in all capitals in parenthesis immediately following the title.

4. DESCRIPTIVE NOTES: If appropriate, enter the type of report, e.g., interim, progress, summary, annual, or final. Give the inclusive dates when a specific reporting period is covered.

5. AUTHOR(S): Enter the name(s) of author(s) as shown on or in the report. Enter last name, first name, middle initial. If military, show rank and branch of service. The name of the principal author is an absolute minimum requirement.

6. REPORT DATE: Enter the date of the report as day, month, year; or month, year. If more than one date appears on the report, use date of publication.

7a. TOTAL NUMBER OF PAGES: The total page count should follow normal pagination procedures, i.e., enter the number of pages containing information.

7b. NUMBER OF REFERENCES: Enter the total number of references cited in the report.

8a. CONTRACT OR GRANT NUMBER: If appropriate, enter the applicable number of the contract or grant under which the report was written.

8b, 8c, & 8d. PROJECT NUMBER: Enter the appropriate military department identification, such as project number, subproject number, system numbers, task number, etc.

9a. ORIGINATOR'S REPORT NUMBER(S): Enter the official report number by which the document will be identified and controlled by the originating activity. This number must be unique to this report.

9b. OTHER REPORT NUMBER(S): If the report has been assigned any other report numbers *(either by the originator or by the sponsor)*, also enter this number(s).

10. AVAILABILITY/LIMITATION NOTICES: Enter any limitations on further dissemination of the report, other than those imposed by security classification, using standard statements such as:

(1) "Qualified requesters may obtain copies of this report from DDC."

(2) "Foreign announcement and dissemination of this report by DDC is not authorized."

(3) "U. S. Government agencies may obtain copies of this report directly from DDC. Other qualified DDC users shall request through _____."

(4) "U. S. military agencies may obtain copies of this report directly from DDC. Other qualified users shall request through _____."

(5) "All distribution of this report is controlled. Qualified DDC users shall request through _____."

If the report has been furnished to the Office of Technical Services, Department of Commerce, for sale to the public, indicate this fact and enter the price, if known.

11. SUPPLEMENTARY NOTES: Use for additional explanatory notes.

12. SPONSORING MILITARY ACTIVITY: Enter the name of the departmental project office or laboratory sponsoring *(paying for)* the research and development. Include address.

13. ABSTRACT: Enter an abstract giving a brief and factual summary of the document indicative of the report, even though it may also appear elsewhere in the body of the technical report. If additional space is required, a continuation sheet shall be attached.

It is highly desirable that the abstract of classified reports be unclassified. Each paragraph of the abstract shall end with an indication of the military security classification of the information in the paragraph, represented as *(TS)*, *(S)*, *(C)*, or *(U)*.

There is no limitation on the length of the abstract. However, the suggested length is from 150 to 225 words.

14. KEY WORDS: Key words are technically meaningful terms or short phrases that characterize a report and may be used as index entries for cataloging the report. Key words must be selected so that no security classification is required. Identifiers, such as equipment model designation, trade name, military project code name, geographic location, may be used as key words but will be followed by an indication of technical context. The assignment of links, roles, and weights is optional.